the highest-lying minimum (C_2 singlet silicon–silicon bond-broken diradical). Given the difference in bond energies for normal C–C single bonds (~88 kcal/mol)[41] and Si–Si single bonds (~74 kcal/mol),[42] one might expect the silicon–silicon diradicals to be lower lying than the carbon–carbon diradicals by ~14 kcal/mol. There are several factors which could explain why the carbon–carbon and silicon–silicon diradicals lie so close to each other. First there are steric effects. As noted above, the gauche silicon–silicon diradicals are more crowded than the gauche carbon–carbon diradicals. The magnitude of the steric effect can be seen by comparing the relative energies of the gauche and trans singlet minima. The trans silicon–silicon bond-broken diradical lies 1.0 kcal/mol lower in energy than the trans carbon–carbon diradical, but the gauche carbon–carbon diradical is 2.3 kcal/mol lower lying than the gauche silicon–silicon diradical. Second, there is the stabilization of the carbon radicals by the β silicons. This β silicon effect has been shown to stabilize carbon radicals by approximately 3 kcal/mol;[43] thus in the case one would expect the carbon–carbon diradical to be stabilized by ~6 kcal/mol relative to the silicon–silicon diradical. Finally, steric effects in 1,2-DSCB would be expected to destabilize the C–C bond relative to the Si–Si bond, and this destabilization is manifested in the unusually long C–C bond in 1,2-DSCB.

(41) Wagman, D. D.; Evans, W. H.; Parker, V. B.; Schumm, R. H.; Halow, I.; Bailey, S. M.; Churney, K. L.; Nuttall, R. L. *J. Phys. Chem. Ref. Data* **1982**, *11*, *Suppl. 2*.
(42) Walsh, R. *The Chemistry of Organic Silicon Compounds*; Patai, S., Rappoport, Z., Eds.; Wiley: New York, 1989; pp 371–391.
(43) Walsh, R. *Pure Appl. Chem.* **1987**, *59*, 69.

Based on our DZ + d SCF results, one would predict the head-to-head dimerization reaction to pass through a multistep mechanism involving first formation of a carbon–carbon bond-broken diradical intermediate, followed by ring closure. This prediction is consistent with what is known experimentally about the head-to-head surface.[2,7,10] Unfortunately, we have been unable to find a transition state linking the carbon–carbon diradical with two separated silaethylene molecules. Such a transition state, presumably, would require a multiconfiguration SCF treatment to be adequately described.

Concluding Remarks

The results we have presented lend credence to what has been long hypothesized, that the head-to-tail dimerization of silaethylene is a concerted 2S + 2S reaction despite this reaction normally being forbidden, and that the head-to-head dimerization reaction is a multistep process involving a diradical intermediate. These findings are consistent with the simple arguments presented in the Introduction concerning relaxation of orbital symmetry. Our results, however, cast little light on the question of why the head-to-head reaction is favored over the head-to-tail in some instances. Certainly this is fertile ground for further theoretical and experimental investigation.

Acknowledgment. This research was supported by the U.S. National Science Foundation, Grant CHE-8718469. We thank Lloyd Colegrove and Jaan Laane for helpful discussions.

Registry No. 1,3-DSCB, 287-55-8; 1,2-DSCB, 14151-37-2; silaethylene, 51067-84-6.

Effect of Bond Multiplicity upon Hydrogen Bonding and Proton Transfers. Double Bonded Atoms

Steve Scheiner* and Lan Wang

Contribution from the Department of Chemistry and Biochemistry, Southern Illinois University, Carbondale, Illinois 62901. *Received October 21, 1991*

Abstract: Ab initio methods are used to study the interactions between $H_2C{=}CH_2$ and $H_2C{=}NH$ and their deprotonated anions. $(H_2CCH{-}H{\cdots}CHCH_2)^-$ is the most weakly bound with a complexation energy of 5.6 kcal/mol at the correlated MP2 level as compared to the stronger interaction of 10.3 for $(HNCH{-}H{\cdots}CHNH)^-$ where the peripheral C atom has been replaced by N. The strongest interaction of 15.4 kcal/mol is observed in $(H_2CN{-}H{\cdots}NCH_2)^-$ where N atoms participate directly in the H-bond. $(H_2CCH{-}H{\cdots}CHCH_2)^-$ contains the longest intermolecular separation while the N···N distance in the latter complex is the shortest. This separation between subunits undergoes a contraction between 0.5 and 0.9 Å as the proton reaches the transfer midpoint. The highest proton transfer barrier of 13 kcal/mol is observed for $(H_2CCH{-}H{\cdots}CHCH_2)^-$. In contrast, the small barrier in $(H_2CN{-}H{\cdots}NCH_2)^-$ is eliminated altogether when zero-point vibrations are considered. Transfer rates are computed using modified RRKM theory. These results are placed within the broader context of other complexes in which the atoms participating in the H-bond are single- and triple-bonded within their respective subunits so as to arrive at systematic conclusions regarding the effects of such multiple bonding upon the energetics of H-bond formation and proton transfer.

Introduction

The distinction in proton transfer properties between "normal" (N or O) acids on one hand, and C-acids, on the other, has been well documented in the literature over the years.[1-4] Differences that have been noted include much slower transfers between C atoms and Brønsted plots that remain linear over long stretches of pK. Among the explanations that have been offered are changes in hybridization (and slow ensuing geometry adjustments) that accompany proton transfers between C atoms, the poorer ability of C-acids to form H-bonds, and the necessity of solvent molecules to reorganize themselves in the transition state.

In an effort to identify unambiguously the underlying reason for these differences, ab initio calculations were recently carried out on a set of small molecules whose hybridization is well defined and whose small sizes preclude significant changes in internal geometry.[5] Moreover, the systems were studied in the absence of any solvent molecules and their complicating effects. The molecules studied there were HCCH and HCN, each of which contain a triple bond and at least nominal sp hybridization. The calculations revealed that a strong C-acid like HCN does indeed

(1) Jones, J. R. *The Ionization of Carbon Acids*; Academic Press: New York, 1973. Eigen, M. *Angew. Chem., Int. Ed. Engl.* **1964**, *3*, 1. Bell, R. P. *The Proton in Chemistry*; Cornell University Press: Ithaca, NY, 1973.
(2) Bednar, R. A.; Jencks, W. P. *J. Am. Chem. Soc.* **1985**, *107*, 7117, 7126, 7135.
(3) Farneth, W. E.; Brauman, J. I. *J. Am. Chem. Soc.* **1976**, *98*, 7891. Han, C. C.; Dodd, J. A.; Brauman, J. I. *J. Phys. Chem.* **1986**, *90*, 471.
(4) Koch, H. F. *Acc. Chem. Res.* **1984**, *17*, 137. Kresge, A. J. *Ibid.* **1975**, *8*, 354. Bordwell, R. G.; Boyle, W. J., Jr. *J. Am. Chem. Soc.* **1975**, *97*, 3447.
(5) Cybulski, S. M.; Scheiner, S. *J. Am. Chem. Soc.* **1987**, *109*, 4199.

0002-7863/92/1514-3650$03.00/0

Table I. Deprotonation Energies (kcal/mol)[a]

	SCF		MP2		
	uncorr	corr	uncorr	corr	expt[b]
H_2CCH_2	422.5	422.0	413.7	410.8	415[c]
CH_2NH[d]	412.8	412.5	409.8	406.9	
CH_2NH	404.6	404.3	394.6	391.5	398 ± 5[e]

[a] With (corr) and without (uncorr) BSSE correction; proton being extracted is in italics. [b] Evaluated by subtracting $^5/_2RT$ from measured $\Delta H°$(298 K) and adding change in zero-point vibrational energy from SCF/6-31+G** harmonic force constants. [c] From ref 11. [d] Proton being extracted is cis to NH hydrogen; removal of trans proton requires an additional 6.4 kcal/mol. [e] From ref 12.

function very much like a normal acid in which the proton may be dissociated from an electronegative atom like O or N. The fundamental distinction in proton transfer properties rests primarily in the intrinsic acidity of the molecule.

The present work attempts to probe this question more deeply by extending the set of systems investigated to include molecules containing a double bond. One might expect that if its strongly acidic character allows HC≡N to behave like a "normal" acid, then changing the triple bond to a double bond, as in H_2C=NH, will lower this acidity, and the proton transfer properties of the latter molecule will be intermediate between HCN and weaker C-acids. H_2C=NH is interesting also in that one may consider the deprotonation of the N atom particularly relevant to a number of biological chromophores where protonation of a Schiff base is crucial to the functioning of the protein.[6] We also investigate H_2C=CH_2 which should compare in an analogous manner with HC≡CH, a subject of the earlier work. In summary, upon completion of the work described herein, we are in a position to understand how the multiplicity of the bond affects the proton transfer properties of a given atom.

Theoretical Method

Ab initio calculations were carried out with the GAUSSIAN-82 series of computer codes.[7] For purposes of consistency with the prior data on triply bonded molecules,[5] the fully polarized 6-31+G** basis set, containing a diffuse sp shell on C and N, was used throughout.[8] Geometries were optimized using the gradient procedures contained within the program. Second-order Moller–Plesset perturbation theory (MP2) was applied[9] to evaluate the effects of electron correlation. The basis set superposition error (BSSE) was corrected via the Boys–Bernardi counterpoise technique.[10]

Since we are concerned here primarily with proton transfers, it is essential to consider first the quality of the theoretical approach for treating the deprotonation of each of the molecules. The data in Table I show that, at all levels of theory, it is somewhat more difficult to extract a proton from the C atom of H_2CCH_2 than from H_2CNH. The difference in deprotonation energy is about 8 kcal/mol at the SCF level but drops to half this amount upon inclusion of electron correlation. The NH proton of H_2CNH is more acidic than is the CH proton; its deprotonation energy is 8 kcal/mol smaller at the SCF level but this difference rises to 15 at the MP2 level. It is hence not surprising that CH deprotonation of H_2CNH has not been observed experimentally.

The computed deprotonation energies may be compared to values that have been determined experimentally.[11,12] The values reported in the last column of Table I have been corrected for zero-point vibrations. The corrected MP2 deprotonation energies are smaller than the experimental measurements by 4–6 kcal/mol. Based on other calculations,[13] it is likely that carrying the MP series to fourth order and computing the vibrational energies at the correlated level would reduce the discrepancy between theory and experiment. Another factor which would enhance the agreement would be use of a larger and more polarizable basis set. Altogether, the MP2/6-31+G** level provides a satisfactory treatment of removal of a proton from the molecules of interest; the discrepancy with experiment is small, fairly uniform from one molecule to the next, and understandable from a fundamental perspective.

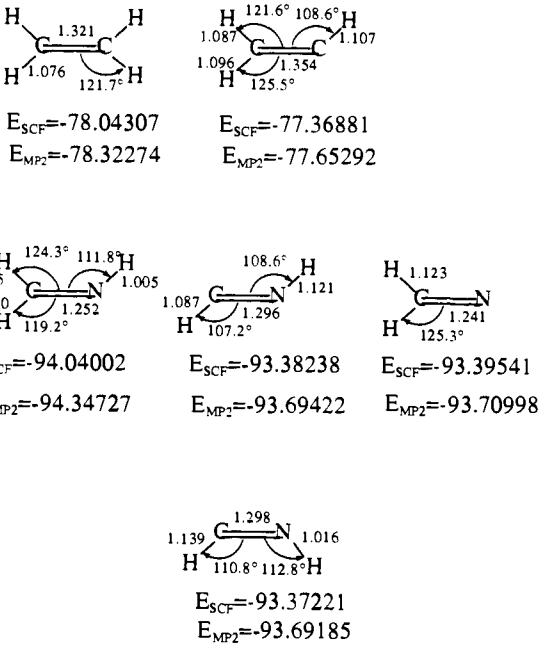

Figure 1. Optimized geometries of neutral molecules (on left) and deprotonated species. Distances are in angstroms, angles in degrees, and energies in hartrees. All species are planar. In addition, H_2CCH_2 belongs to D_{2h} point group; H_2CN^- to C_{2v}.

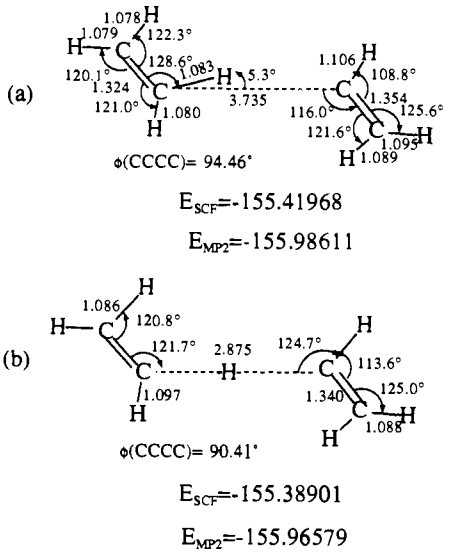

Figure 2. SCF optimized geometries and energies of (a) the complex formed between H_2CCH_2 and H_2CCH^- and (b) the transition state for proton transfer. Distances are in angstroms, angles in degrees, and energies in hartrees. The planes of the two subunits are nearly perpendicular to one another.

Geometries

The geometries of H_2CCH_2 and H_2CNH, along with their deprotonated analogues, were fully optimized at the SCF level.

(6) Braiman, M. S.; Mogi, T.; Marti, T.; Stern, L. J.; Khorana, H. G.; Rothschild, K. J. *Biochemistry* **1988**, *27*, 8516. Lin, S. W.; Mathies, R. A. *Biophys. J.* **1989**, *56*, 653. Polland, H.-J.; Franz, M. A.; Zinth, W.; Kaiser, W.; Kolling, E.; Oesterhelt, D. *Biophys. J.* **1986**, *49*, 651.

(7) Binkley, J. S.; Frisch, M.; Raghavachari, K.; DeFrees, D. J.; Schlegel, H. B.; Whiteside, R. A.; Fluder, E.; Seeger, R.; Pople, J. A. *GAUSSIAN 82*, Release H.; Carnegie-Mellon University: Pittsburgh, PA, 1984.

(8) Hariharan, P. C.; Pople, J. A. *Theor. Chim. Acta* **1973** *28*, 213. Chandresekhar, J.; Andrade, J. G.; Schleyer, P. v. R. *J. Am. Chem. Soc.* **1981**, *103*, 5609.

(9) Pople, J. A.; Binkley, J. S.; Seeger, R. *Int. J. Quantum Chem., QCS* **1976**, *10*, 1. Krishnan, R.; Pople, J. A. *Int. J. Quantum Chem.* **1976**, *14*, 91. Krishnan, R.; Frisch, M. J.; Pople, J. A. *J. Chem. Phys.* **1980**, *72*, 4244.

(10) Boys, S. F.; Bernardi, S. F. *Mol. Phys.* **1970**, *19*, 553.

(11) Kass, S. R.; DePuy, C. H. *J. Org. Chem.* **1985**, *50*, 2874.

(12) DePuy, C. H.; Bierbaum, V. M.; Damrauer, R. *J. Am. Chem. Soc.* **1984**, *106*, 4051.

(13) Del Bene, J. E.; Shavitt, I. *J. Phys. Chem.* **1990**, *94*, 5514. Siggel, M. R. F.; Thomas, T. D.; Saethre, L. J. *J. Am. Chem. Soc.* **1988**, *110*, 91. Ikuta, S.; Nomura, O. *J. Chem. Phys.* **1987**, *87*, 3701. DeFrees, D. J.; McLean, A. D. *J. Comput. Chem.* **1986**, *7*, 321.

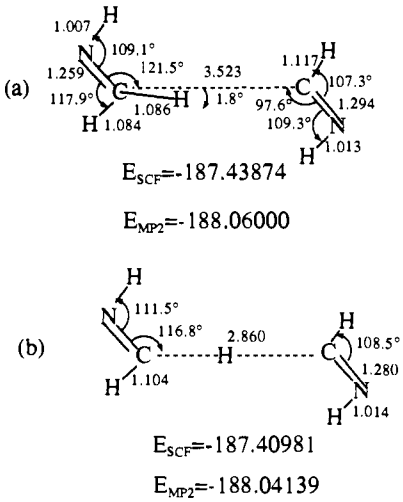

Figure 3. SCF optimized geometries and energies of (a) the complex formed between $HNCH_2$ and $HCNH^-$ and (b) the transition state for proton transfer. All atoms lie in a common plane.

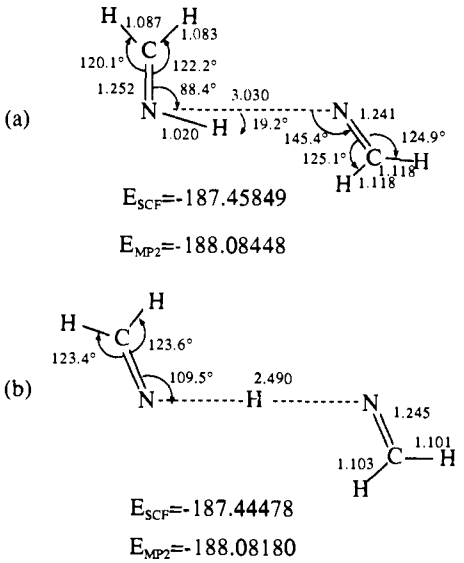

Figure 4. SCF optimized geometries and energies of (a) the complex formed between CH_2NH and NCH_2^- and (b) the transition state for proton transfer. All atoms lie in a common plane.

These geometries, along with the associated SCF and MP2 energies, are reported in Figure 1. It may be noted that the C=N double bond in H_2CNH is shorter than C=C in ethylene. Removal of a CH proton from either neutral molecule leads to elongation of the double bond whereas a contraction is noted when the NH proton is removed from H_2CNH; all remaining X–H bonds become longer following protonation.

The geometries of the various complexes are illustrated in the top part of Figures 2–4. It should first be noted that the fully optimized geometry of $(H_2CCH_2\cdots HCCH_2)^-$ in Figure 2 is not fully planar in that the two subunits are nearly perpendicular to one another. On the other hand, rotation into a fully planar arrangement raises the energy of this complex by less than 0.006 kcal/mol. This planar geometry differs from the nonplanar one depicted in Figure 2 in only a few particulars; the salient features of the structure are basically unchanged. The geometries of the other systems are fully planar. Figure 3 treats the CH···C interaction in $(HNCH_2\cdots CHNH)^-$ where the proton acceptor molecule is in its trans arrangement. If $HCNH^-$ adopts a cis configuration, the CH···C interaction becomes severely distorted due to the stronger basicity of the N atom as compared to carbon. The proton-donating $HNCH_2$ molecule rotates as does the $HCNH^-$ until the bridging proton is closer to the N atom (2.40 Å) than to the carbon (2.80 Å). The greater basicity of the N is revealed also by the binding energy between the two subunits which is 14.9 kcal/mol in the cis complex as compared to 10.3 in trans. The last complex is illustrated in Figure 4a and involves the NH···N interaction.

Table II. Binding Energies (kcal/mol) with and without BSSE Correction

	SCF		MP2[a]	
	uncorr	cor	uncorr	corr
$(H_2CCH_2\cdots CHCH_2)^-$	4.9	4.6	6.6	5.6
$(HNCH_2\cdots CHNH)^-$	10.3	9.8	11.6	10.3
$(H_2CNH\cdots NCH_2)^-$	14.5	13.9	17.1	15.4

[a] Computed using SCF geometries.

In each case, complexation pulls the bridging hydrogen toward the anion, elongating the X–H bond. The longest intermolecular separation X--X is 3.735 Å for the $(H_2CCH_2\text{--}CHCH_2)^-$ complex. This distance diminishes to 3.523 Å in $(HNCH_2\text{--}CHNH)^-$ and 3.030 Å in $(H_2CNH\text{--}NCH_2)^-$.

The bridging proton lies close to the X--X axis in these complexes. The exception occurs in the NH···N system in Figure 4a where there is a 19° nonlinearity. This H-bond distortion energy is probably compensated by the better alignment between the dipole moment of $HNCH_2$ and the negative charge of the NCH_2^- subunit. That is, the dipole moment of $HNCH_2$ is oriented such that its positive end points approximately toward the CH hydrogen on the right in Figure 4a. It is not surprising that this positive charge is drawn toward the negatively charged subunit, thereby distorting the NH···N interaction in the manner shown.[14]

The transition states for proton transfer are presented in the lower halves of Figures 2–4. In all cases the central proton adopts a position directly along the X--X axis. The X--X intermolecular separation is considerably shorter in the transition state as compared to the corresponding complex. The contraction undergone by R(X--X) as a result of half transfer of the proton is 0.86 Å for $(H_2CCH_2\text{--}CHCH_2)^-$, 0.66 Å for $(HNCH_2\text{--}CHNH)^-$, and 0.54 Å for $(H_2CNH\text{--}NCH_2)^-$. These contractions are uniformly larger than the values of 0.545 Å, 0.414 Å, and 0.235 Å calculated previously for the corresponding triply bonded analogues.[5] Half-transfer of the proton results also in a reorientation of the two subunits. For example, the C=C···C angles in $(H_2CCH_2\text{--}CHCH_2)^-$, are 129° and 116° for the proton donor and acceptor subunits, respectively. When the bridging proton lies midway between the C atoms, these angles have changed to 122°. Similar reorientations are noted in the other systems as well.

Energetics

Binding Energies. Table II lists the binding energy of each complex, computed as the difference in total energy between the complex on one hand and the pair of isolated optimized subunits on the other. Results are reported both before and after counterpoise correction of the BSSE.[10] At any level of theory, the binding energies bear a positive correlation with the ease of deprotonation of the proton donor (Table I). That is, the strength of the interaction grows with acidity of the donor molecule. This trend is consistent with patterns noted in the past.[5,15,16]

The data in Table II suggest that correlation has a small effect on the binding of these complexes. Considering those values corrected for BSSE, the MP2 binding energy is greater than the SCF result by 1.0 kcal/mol for $(H_2CCH_2\cdots CHCH_2)^-$, 0.5 for $(HNCH_2\cdots CHNH)^-$, and 1.5 for $(H_2CNH\cdots NCH_2)^-$. The basis set superposition errors to the binding energies are equal to the difference between the values in the corr and uncorr columns of Table II. The total BSSE at the MP2 level amounts to 1.0–1.7 kcal/mol. Of this total, the SCF BSSE varies between 0.3 and 0.6 kcal/mol as compared to a correlation component of 0.7–1.1 kcal/mol.

Proton-Transfer Barriers. The difference in energy between the complexes illustrated in Figures 2a–4a and the transition states

(14) Cybulski, S. M.; Scheiner, S. *J. Phys. Chem.* **1990**, *94*, 6106.
(15) Latajka, Z.; Scheiner, S. *Int. J. Quantum Chem.* **1986**, *29*, 285.
(16) Redfern, P.; Scheiner, S. *J. Phys. Chem.* **1986**, *90*, 2969.

Table III. Energy Barriers to Proton Transfer (kcal/mol)

	SCF	MP2[a]
$(H_2CCH_2\text{--}CHCH_2)^-$	19.2	12.8
$(HNCH_2\text{--}CHNH)^-$	18.2	11.7
$(H_2CNH\text{--}NCH_2)^-$	8.6	1.7

[a] Computed using SCF geometries.

Table IV. Zero-Point Vibrational Energies (kcal/mol) Calculated with 6-31+G Basis Set

	L = H	L = D
L_2CCL^-	24.11	18.43
L_2CCL_2	34.52	26.22
NCL_2^-	16.22	12.70
$LNCL^-$	17.15	13.23
$LNCL_2$	27.07	20.73
$(H_2CCH_2\text{--}CHCH_2)^-$	59.31	45.19
$(H_2CCH\text{--}H\text{--}CHCH_2)^-$	56.12	43.09
$(HNCH_2\text{--}CHNH)^-$	45.45	34.99
$(HNCH\text{--}H\text{--}CHNH)^-$	42.39	32.94
$(H_2CNH\text{--}NCH_2)^-$	44.98	34.72
$(H_2CN\text{--}H\text{--}NCH_2)^-$	41.77	32.57

for proton transfer in Figures 2b–4b correspond to the transfer barriers, $E^\dagger$. These barriers are listed in Table III at both the SCF and MP2 levels. It is first clear that the correlated barriers in the last column are considerably smaller than the SCF barriers, a feature that has been noted numerous times previously for other systems.[5,15,17,18] The correlation-induced barrier lowering is fairly uniform from one complex to the next, varying in the relatively narrow range of 6.4–6.9 kcal/mol. While it is possible in principle that reoptimization of the geometries of the transition state and energy minimum at the correlated level might alter the energetics of proton transfer, our earlier work with the triply bonded analogues[5] and other systems[15] has provided evidence that such changes are quite minimal.

At any level of theory, the transfer barriers between two C atoms (first two rows) are considerably higher than the inter-nitrogen transfer barrier in the last row. Within the former category of intercarbon transfer, the barrier for $(H_2CCH_2\cdots CHCH_2)^-$ is 1.1 kcal/mol higher than that for $(HNCH_2\cdots CHNH)^-$, indicating a small influence from the portion of the molecule not participating directly in the H-bond. There is a correlation between the barriers and the deprotonation energies of the monomers listed in Table I which will be commented on in greater detail below.

Vibrational Frequencies. A vibrational analysis was carried out within the context of harmonic frequencies for each monomer and complex described above. Reported in Table IV are the sum totals of zero-point vibrational energy (ZPVE) for each of these species, with hydrogen as both protium and deuterium. (Computational limitations precluded full frequency evaluations of the complexes; hence data in Table IV were obtained with the 6-31+G set.) Comparison of the data supports an observation made previously[5] for the triple-bonded analogues: each substitution of a H atom by D produces a 2-kcal/mol decrease in the total zero-point energy.

From the lower half of the table, one may note that the ZPVE of each transition state to proton transfer is some 3 kcal/mol less than that for the equilibrium geometry preceding it in the table (ca. 2 kcal/mol for the deuterated species). This difference accounts for a ZPVE-induced drop in the transfer barrier by a like amount. The vibrational effects are also responsible for decreases in the binding energies by some 1 to 2 kcal/mol.

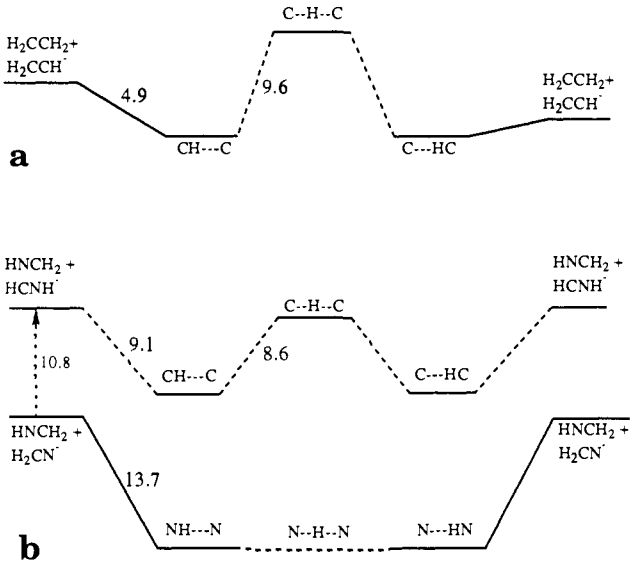

Figure 5. Energy profiles (in kcal/mol) for reaction of (a) H_2CCH_2 + H_2CCH^- and (b) $HNCH_2$ + either H_2CN^- or $HCNH^-$. All energy differences were computed at the MP2 level and have been corrected for zero-point vibrations; superposition errors have been removed from association energies by counterpoise. The small barrier to inter-nitrogen proton transfer vanishes when vibrational effects are included.

The frequencies corresponding to the bending of the bridging proton off of the H-bond axis vary between 1584 and 1754 cm^{-1} for the three transition states to transfer. However, there is no clear relationship between the "flexibility" associated with these frequencies and the strength of the H-bonding interaction.

Extension of the basis set appears to lead to only minor changes in these frequencies. After reintroduction of the polarization functions back into the basis set (6-31+G**), the zero-point energies of the monomers in the first five rows of Table IV were recomputed. Only very small changes were observed, all less than 0.4 kcal/mol.

Reaction Profiles. Combination of the above energetics with the vibrational frequencies allows one to describe the various minimum energy pathways for proton transfer. Figure 5a illustrates the situation for the H_2CCH_2 + $CHCH_2^-$ system. The complexation energy is 4.9 kcal/mol, following correction of the MP2 result for basis set superposition and zero-point vibrational energies. In order to transfer from one subunit to the other within the $(H_2CCH\cdots CHCH_2)^-$ complex, the central proton must surmount an energy barrier of 9.6 kcal/mol, again corrected for ZPVE.

Comparison with Figure 5b reveals that the binding energies are significantly larger and the proton transfer barriers lower when the CH_2NH molecule is combined with either of the deprotonated anions CH_2N^- or $NHCH^-$. Either the C–H or N–H proton of CH_2NH may act as bridging hydrogen; hence, two complexes are possible in principle with either anion. In the case of $NHCH^-$, the C atom is the better proton acceptor. The CH--C complex is formed when the C–H group of CH_2NH acts as donor. Following correction of zero-point vibrations, this complex is bound by 9.1 kcal/mol relative to the individual monomers as shown in Figure 5b. The subsequent barrier for proton transfer is only 0.5 kcal less than this amount. The NH--C complex, which occurs if the NH group of CH_2NH acts as proton donor, is slightly more stable than CH--C (by 2.6 kcal). However, this complex is not included in Figure 5b since the ensuing transfer, which should lead to the N--HC complex, spontaneously rearranges to the NH--N geometry. Considering next the N atom of CH_2N^- as the proton acceptor, the NH group of CH_2NH is the best proton donor. The NH--N complex is bound by 13.7 kcal/mol, the strongest of those considered here. As illustrated in Figure 5b, zero-point vibrations cause the proton-transfer barrier to vanish.

(17) Scheiner, S.; Szczesniak, M. M.; Bigham, L. D. *Int. J. Quantum Chem.* **1983**, *23*, 739. Scheiner, S.; Harding, L. B. *J. Am. Chem. Soc.* **1981**, *103*, 2169. Latajka, Z.; Scheiner, S. *J. Mol. Struct. (THEOCHEM)* **1991**, *234*, 373.

(18) Gejji, S. P.; Taurian, O. E.; Lunell, S. *J. Phys. Chem.* **1990**, *94*, 4449. Bosch, E.; Moreno, M.; Lluch, J. M.; Bertran, J. *Chem. Phys.* **1990**, *148*, 77. Truong, T. N.; McCammon, J. A. *J. Am. Chem. Soc.* **1991**, *113*, 7504. Shida, N.; Barbara, P. F.; Almlöf, J. E. *J. Chem. Phys.* **1989**, *91*, 4061. Frisch, M. J.; Scheiner, A. C.; Schaefer, H. F., III; Binkley, J. S. *J. Chem. Phys.* **1985**, *82*, 4194. Sauer, J.; Kölmel, C. M.; Hill, J.-R.; Ahlrichs, R. *Chem. Phys.* **1989**, *164*, 193. Hodoscek, M.; Hadzi, D. *J. Mol. Struct. (THEOCHEM)* **1990**, *209*, 411.

Table V. Thermodynamic Properties[a] Computed for Binding Reactions AH + B^- → $(AH\cdot\cdot B)^-$

	1 K	10 K	100 K	300 K	500 K	1000 K
			$\Delta H°$ (kcal/mol)			
CCH··CC	−5.3	−5.3	−5.4	−4.8	−4.0	−2.1
NCH··CN	−9.1	−9.2	−9.6	−9.6	−9.4	−8.6
CNH··NC	−13.8	−13.9	−14.2	−13.8	−13.2	−11.5
			$\Delta S°$ (cal/K mol)			
CCH··CC	−2.6	−19.1	−24.3	−21.0	−19.2	−16.5
NCH··CN	−1.9	−20.2	−34.0	−34.4	−33.8	−32.8
CNH··NC	−2.4	−20.7	−31.8	−30.0	−28.4	−26.0
			$\Delta G°$ (kcal/mol)			
CCH··CC	−5.2	−5.1	−2.9	1.6	5.6	14.4
NCH··CN	−9.1	−8.8	−6.2	0.7	7.5	24.1
CNH··NC	−13.8	−13.7	−11.0	−4.8	1.0	14.6

[a] Standard state is ideal gas at 1 atm.

The energy barrier for transfer of a proton between the two C atoms of $(HNCH_2\cdot\cdot CHNH)^-$ is 1.0 less than in $(H_2CCH\cdots CHCH_2)^-$.

While the profiles detailed in Figure 5 illustrate the lowest energy path which will accomplish the proton transfer, there is no guarantee that the reaction will, in fact, follow this pathway. Indeed, there is evidence[19] that transfer of a light atom between two heavy species will detour significantly from this pathway, such that the highest energy point on the dominant tunneling path (the critical configuration) may be higher that the saddle point energies in Figure 5.

Thermochemistry. All of the preceding energetics pertain to 0 K. Extrapolation of the data to higher temperatures is possible through standard thermodynamic formulas that incorporate the vibrational frequencies of the various species. The properties of the binding processes are displayed in Table V for each of the complexes with identical donor and acceptor.

One may note from the upper portion of the table that the binding enthalpies are fairly insensitive to temperature although there is a small reduction in the magnitude of these complexation energies as the temperature rises. As in many cases of this sort, the low-frequency intermolecular modes of the complex become increasingly populated as the temperature rises, increasing its total energy. In contrast, the more nearly temperature-independent energy of the monomers, without such low-frequency vibrations, causes their average energy to remain relatively static, resulting in a diminished binding enthalpy with higher temperature.

The negative values of $\Delta S°$ indicate principally the loss of translational and rotational freedom upon binding a pair of freely rotating subunits into a single complex. As the temperature climbs beyond about 100–300 K, the entropy of binding begins to become less negative. This change reflects the greater accessibility of the aforementioned low-frequency intermolecular vibrations of the complexes and the accompanying broader distribution of vibrational quanta.

The Gibbs free energies reported in the last section of Table V reflect only $\Delta H°$ at low temperatures. As T increases, the negative entropies of binding become increasingly more important such that $\Delta G°$ becomes positive. The thermoneutrality point is reached at about 500 K for $(HNCH_2\cdots CHNH)^-$ but only 200 K for the more weakly bound $(H_2CCH\cdots CHCH_2)^-$. One further point of interest concerns the observation that the relative order of stability of the three complexes which one finds at 0 K is unchanged at higher temperatures and is true whether one considers $\Delta H°$ or $\Delta G°$.

Kinetics of Proton Transfer

One common means of estimating the rate of a reaction is via RRKM theory.[20] In the case of a proton transfer, however, it is essential that some consideration be included of the ability of a proton to tunnel through a barrier. In order to account for this phenomenon, a number of authors have suggested[21] that the sum of the transmission coefficients be substituted for the number of states of the activated complex when the energy level lies below the top of the barrier. This concept has been incorporated by us[22] into the standard RRKM program of Hase and Bunker[23] such that our modified program includes tunneling explicitly. Following the recommendation of Miller,[21d] the quantum mechanical barrier was fit to an Eckart potential via its height and imaginary frequency. (Because corner-cutting was neglected, the rates computed here are likely to serve as a lower limit to the true magnitude of tunneling.[19]) By Boltzmann summation of the microcanonical data, one arrives at the transfer rate as a function of T. Tests of this procedure and comparison with experiment and conventional transition state theory suggest this approach can provide reasonable results.[5,22,24]

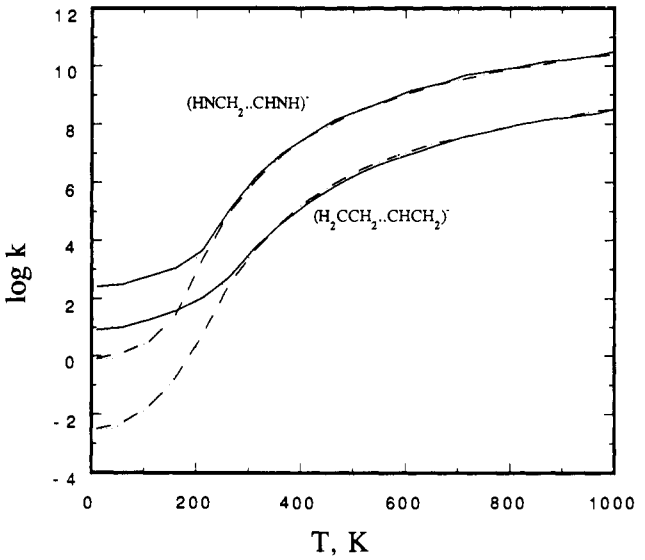

Figure 6. Calculated rate constants for proton transfer (s^{-1}). Broken curves refer to fully deuterated complexes.

The temperature dependence of the transfer rate for the $(H_2CCH\cdots CHCH_2)^-$ and $(HNCH_2\cdots CHNH)^-$ complexes are illustrated as the solid curves in Figure 6; results for the fully deuterated analogues are represented by the broken curves. Consistent with other systems examined in this manner, the curves are faily flat at very low temperatures where the process is dom-

(19) Bondi, D. K.; Connor, J. N. L.; Garrett, B. C.; Truhlar, D. G. *J. Chem. Phys.* **1983**, *78*, 5981. Kreevoy, M. M.; Ostovic, D.; Truhlar, D. G.; Garrett, B. C. *J. Phys. Chem.* **1986**, *90*, 3766.

(20) Robinson, P. J.; Holbrook, K. A. *Unimolecular Reactions*; Wiley-Interscience: New York, 1972. Forst, W. *Theory of Unimolecular Reactions*; Academic: New York, 1973. Hase, W. L. *Acc. Chem. Res.* **1983**, *16*, 258.

(21) (a) Marcus, R. A. *J. Chem. Phys.* **1965**, *43*, 1598. (b) Marcus, R. A. In *Investigation of Rates and Mechanisms of Reactions*, 3rd ed.; Lewis, E. S., Ed.; Wiley-Interscience: New York, 1974; Part I, p 13. (c) Garrett, B. C.; Truhlar, D. G. *J. Phys. Chem.* 1979, *83*, 1079. (d) Miller, W. H. *J. Am. Chem. Soc.* **1979**, *101*, 6801.

(22) Scheiner, S.; Latajka, Z. *J. Phys. Chem.* **1987**, *91*, 724.

(23) Hase, W. L.; Bunker, D. L. *QCPE* **1973**, *11*, 234.

(24) Isaacson, A.; Wang, L.; Scheiner, S. To be published.

Table VI. Comparison of Properties Computed for Complexes Studied

	$(H_2CCH-H\cdots CHCH_2)^-$	$(HNCH-H\cdots CHNH)^-$	$(H_2CN-H\cdots NCH_2)^-$
R_{eq}, Å	3.735	3.523	3.030
R_{ts}, Å	2.875	2.860	2.490
ΔR, Å	−0.86	−0.66	−0.54
ΔE_{MP2}, kcal/mol	5.6	10.3	15.4
$E^{\dagger}_{MP2}$, kcal/mol	12.8	11.7	1.7

inated by tunneling. As T increases above 100 K or so, however, the rate begins to climb quickly as energy levels above the transfer barrier become more heavily populated, and classical over-the-barrier transfers become more important. Finally at high temperatures, the rates level off as they approach their asymptotes.

It is of interest to compare the transfer rates in Figure 6 with the previously calculated data for the triply bonded analogues.[5] Beginning with the hydrocarbon systems, the ZPVE-corrected energy barrier of 9.6 kcal/mol for $(H_2C{=}CH\cdots CH{=}CH_2)^-$ is nearly double that calculated previously (5.1) for $(HC{\equiv}CH\cdots C{\equiv}CH)^-$. Since tunneling rates are highly dependent upon barrier height, it is not surprising that the low-temperature limit of the transfer rate in the doubly bonded system is 8 orders of magnitude slower than in $(HC{\equiv}CH\cdots C{\equiv}CH)^-$. Comparison of $(HN{=}CH_2\cdots CH{=}NH)^-$ with $(N{\equiv}CH\cdots C{\equiv}N)^-$ shows again a higher barrier in the former case (8.6 versus 2.5 kcal/mol) and a tunneling rate approximately 8 orders of magnitude slower. On the other extreme, in the limit of high temperature, the doubly and triply bonded systems show much smaller differences and little dependence to deuterium versus protium, all converging toward rates on the order of 10^9–10^{12}.

The dashed curves in Figure 6, representing the deuterated systems, are fairly close to the solid curves of the protiated analogues at high temperatures. However, as T diminishes and as tunneling makes a progressively larger contribution to the overall process, the D^+ transfer becomes markedly slower than proton transfer.

Summary and Discussion

The complexes studied here show systematic trends that are useful in attempts to understand hydrogen-bonded systems and the proton transfers that occur within them. The salient data are compiled in Table VI where it may be seen that the length of the H-bond in the equilibrium structures (first row) diminishes from left to right. A similar reduction is observed in the intermolecular separations in the transition states as well. The third row of the table lists the contraction that occurs as a result of the proton moving halfway from the donor to acceptor atom, i.e., from equilibrium geometry to transition state. The magnitude of this reduction diminishes from 0.86 Å for transfer between ethylene species to 0.54 Å for transfer between N atoms. Our best estimate of the hydrogen bond energy of each complex, computed at the MP2 level and corrected for basis set superposition error, is reported in the next row of Table VI. It is apparent that the most strongly bound complexes are also those with the shortest H-bond length as well as the smallest reduction in R as a result of half-proton transfer. The last row reveals an inverse correlation between the height of the energy barrier to proton transfer and the strength of the binding within the complex. Comparison with Table I suggests an additional link in that the most strongly bound complexes are those for which extraction of a proton from the parent neutral molecule is most facile. That is, those molecules with the smallest deprotonation energy (most acidic) are associated with stronger H-bonds.

Table VII. Comparison of Properties Computed for C–H···C H-Bonded Complexes

	$(H_3C-H\cdots CH_3)^-$ [a]	$(H_2C{=}CH-H\cdots CH{=}CH_2)^-$	$(HC{\equiv}C-H\cdots C{\equiv}CH)^-$ [b]
R_{eq}, Å	4.43	3.74	3.35
R_{ts}, Å	2.91	2.88	2.81
ΔR, Å	−1.52	−0.86	−0.54
ΔE_{SCF}, kcal/mol	1.0	4.6	9.8
ΔE_{MP2}, kcal/mol	2.0	5.6	10.8
$E^{\dagger}_{SCF}$, kcal/mol	22	19	13
$E^{\dagger}_{MP2}$, kcal/mol	12	13	8

[a] From ref 15, using 6-31G**+p(C) basis set. [b] From ref 5.

Table VII places these results within the larger framework of systems representing other types of bonding within the various subunits. Whereas all the atoms involved in H-bonding and proton transfers investigated here are doubly bonded within their individual subunit, the C atoms are involved in triple bonds in our earlier study of $(HC{\equiv}C\text{-}H\cdots C{\equiv}CH)^-$.[5] In addition, there are only single bonds to the C atoms in $(H_3C\text{-}H\cdots CH_3)^-$, a system also studied previously by comparable theoretical methods.[15] It is readily apparent from inspection of Table VII that the increased multiplicity of bonding is tantamount to greater electronegativity as discussed above. That is, upon going from singly to doubly to triply bonded C atoms, one may observe contraction in the intermolecular C···C separation in both the equilibrium and transition state structures, as well as reduction in the C···C contraction associated with half-proton transfer. Also evident in Table VI is the increasing H-bond strength ΔE at either SCF or MP2 level. (It is intriguing to note that in all three cases, the correlated interaction energy exceeds the SCF value by 1.0 kcal/mol.) Finally, the proton-transfer barriers are lowered as the multiplicity of the bonding to the C atom increases. Electron correlation lowers all barriers by amounts ranging between 5 and 10 kcal/mol. All of these trends are consistent with the increasing electronegativity associated with a triply bonded C atom as compared to double or single bonds, a trend borne out by experimental and computed deprotonation energies, as well as simple arguments based upon greater proportional s/p character of the hybrid orbitals for triple bonds.

Acknowledgment. We are grateful to Dr. S. M. Cybulski for help with the initial calculations. This work was supported by the National Institutes of Health (GM29391).

Registry No. $H_2C{=}CH_2$, 74-85-1; $H_2C{=}CH^-$, 25012-81-1; $H_2C{=}NH$, 2053-29-4; $NH{=}CH^-$, 90623-30-6; $H_2C{=}N^-$, 28892-56-0; D_2, 7782-39-0.